Molecular and Isotope Analyses of Organic Matter in a Primitive Clast in the Zag H Chondrite

*Yoko Kebukawa[1], Motoo Ito[2], Michael E. Zolensky[3], Aiko Nakato[4], Hiroki Suga[5], Yoshio Takahashi[6], Takeichi Takeichi[7,8], Kazuhiko Mase[7,8], Queenie H. S. Chan[9], Marc Fries[3], Kensei Kobayashi[1]

1. Faculty of Engineering, Yokohama National University, 2. Kochi Institute for Core Sample Research JAMSTEC, 3. ARES, NASA Johnson Space Center, 4. Kyoto University, Division of Earth and Planetary Sciences, 5. Graduate School of Science, Hiroshima University, 6. Department of Earth and Planetary Science, Graduate School of Science, The University of Tokyo, 7. Institute of Materials Structure Science, High-Energy Accelerator Research Organization (KEK), 8. Department of Materials Structure Science, SOKENDAI (The Graduate University for Advanced Studies), 9. Planetary and Space Sciences, Department of Physical Sciences, The Open University

The Zag meteorite is a halite-bearing H3-6 chondrite [1]. The Zag contains xenolithic clast with abundant organic matter which was proposed to be originated from Ceres [2,3]. Here we report coordinated organic analyses by STXM-XANES and NanoSIMS, in order to understand the nature and origin of the organic matter. Our systematic research of the Zag clast may also provide an important linkage to the recent remote sensing observations obtained by the DAWN mission to Ceres [e.g., 4,5].
Carbon-rich areas were located in the clast grains separated from the Zag meteorite with SEM-EDS, and then lift-out sections were prepared with a FIB instrument. C, N, O-X-ray absorption near-edge structure (C,N,O-XANES) spectra of the sections (~100 nm-thick) were obtained using scanning transmission X-ray microscopes (STXM) on beamline 5.3.2.2 at Advanced Light Source, Lawrence Berkeley National Laboratory, and BL-13A at the Photon Factory, KEK. Subsequently, H, C, N, O isotopic images were collected using a CAMECA NanoSIMS 50L ion microprobe.
The STXM elemental map of C-rich region of the Zag clast shows that sub-micrometer organic grains were scattered over the FIB section, some of which have a vein-like structure. The organic matter was somewhat associated with Fe (probably Fe-sulfides). The Fe (+Ni) and C association was also observed in the clasts in Sharps (H3.4) chondrite, suggesting a potential of catalytic gas-solid reactions such as Fischer-Tropsch type (FTT) synthesis [6,7].
C-XANES spectra of the organic grains showed large peaks at 285.2 eV assigned to aromatic carbon, and at 290.3 eV assigned to carbonate (either organic or inorganic), with some features at 287.4 eV (enol C=C-OH), and 287.9 eV (aliphatic), and 288.8 eV (carboxyl). The C-XANES spectra have some similarity with organic matter from Comet Wild 2, rather than with primitive chondritic IOM [8], except for the abundant carbonate in the Zag clast.
NanoSIMS isotope imaging analyses revealed that δ^{15}N and δD have highly heterogeneous distributions within the organic matter. The average δ^{15}N value was 393 ±82 ‰with a hot spot (2639 ±722 ‰), and the average δD value was 813 ±206 ‰with a hot spot (4,150 ±1,710 ‰). The δ^{15}N was similar to the value of insoluble organic matter (IOM) from Bells (an unusual CM chondrite) and CRs, although δD was less than these IOM [9]. It may indicate that some hydrogen have been exchanged with isotopically light water in the clast parent body.
Both molecular structure and isotopic signatures indicated highly pristine (less altered) nature of organic matter in the clast, and it may be related to cometary organics and/or primitive chondritic IOM.

References: [1] Zolensky M. E. et al. (1999) *Science, 285,* 1377–1379. [2] Fries M. et al. (2013) *76th MetSoc,* Abstract #5266. [3] Zolensky M. E. et al. (2015) *78th MetSoc,* Abstract #5270. [4] Nathues A. et al. (2015) *Nature, 528,* 237–240. [5] De Sanctis M. C. et al. (2015) *Nature, 528,* 241–244. [6] Brearley A.

J. (1990) *Geochim. Cosmochim. Acta, 54,* 831–850. [7] Kebukawa Y. et al. (2017) *Geochim. Cosmochim. Acta, 196,* 74–101. [8] Cody G. D. et al. (2008) *Meteorit. & Planet. Sci., 43,* 353-365. [9] Alexander C. M. O' D. et al. (2007) *Geochim. Cosmochim. Acta, 71,* 4380–4403.

Keywords: Meteorite, Organic matter, Isotope

Oxygen isotopic ratio of the primordial water in CM chondrites

*Wataru Fujiya[1]

1. Ibaraki University, College of Science

CM chondrites are aqueously altered to various degrees in their parent body. Water ice accreted on the CM parent body reacted with primary anhydrous rock and organic matter producing secondary minerals. The O and H isotopic ratios of the primordial water are key constraints on its origin, however, they are still not well-constrained due to complex isotope exchange between water, rock, and organic matter during the aqueous alteration. Here I investigate the O isotopic ratio of the primordial water in CM chondrites based on bulk O isotopic ratios of CM chondrites and H abundances of their phyllosilicate. Most of the O and H data are from Clayton and Mayeda (1999) and Alexadner et al. (2013).
CM Falls show an apparent correlation between bulk $\delta^{18}O$ values and H abundances of their phyllosilicate. The regression line of the CM Falls passes through the representative compositions of anhydrous silicate and phyllosilicate matrix in CM chondrites, indicating a mixing line between these two components as endmembers. This well-defined mixing line strongly indicates that the O isotopic ratios of bulk CM chondrites reflect variable amounts of anhydrous silicate and phyllosilicate, i.e., degrees of alteration. A consequence from the mixing line is that phyllosilicate in CM chondrites must have a common O isotopic ratio irrespective of their alteration degrees.
Oxygen isotopic ratios of phyllosilicate are dependent not only on alteration degrees but also on water/rock ratios. Here alteration degrees (f) are evaluated as fraction of anhydrous silicate reacted, and water/rock ratios (x) are expressed as ratios of O moles in water to those in anhydrous rock. In a closed system alteration model by Clayton and Mayeda (1999), O isotopic ratios of phyllosilicate are expressed as a function of f/x based on a mass balance calculation of water, anhydrous silicate, and phyllosilicate. If there is enough water to completely alter anhydrous rock (i.e., large x), then f can range from 0 to 1. In contrast, if anhydrous rock remains after complete consumption of water (i.e., small x), f cannot reach to 1 but only take values smaller than 1 depending on x. Thus, f/x values have a maximum, when water is completely consumed by the aqueous alteration and O isotopic ratios of phyllosilicate should be the same. Given apparent occurrence of anhydrous silicate that remains unaltered, water/rock ratios are likely a limiting factor for the alteration degrees of CM chondrites. Complete water consumption is thus the most straightforward explanation for the similar O isotopic ratios inferred for CM phyllosilicate. Neither alteration temperatures nor hydration reaction considered in the calculation does this conclusion rely on. If no water remained in the system after the aqueous alteration, water/rock ratios of individual CM chondrites can be deduced from H abundances of their phyllosilicate. The deduced x values range from 0.11 to 0.29 (0.19 –0.49 by volume ratios). The variable water/rock ratios would suggest heterogeneous water ice accretion on the CM chondrite parent body.
An important implication from this scenario is the O isotopic ratio of the primordial water. In an O three-isotope plot, the O isotopic ratio of CM phyllosilicate should be on the line connecting the O isotopic ratios of the anhydrous silicate and the primordial water. Based on the mass-balance calculation by Clayton and Mayeda (1999), the inferred $\delta^{18}O$ and $\delta^{17}O$ values of the primordial water are ~65 and ~43 ‰, respectively. These estimates depend on hydration reaction considered in the calculation.

Keywords: Aqueous alteration, CM chondrite, Oxygen isotopic ratio, Primordial water

Carbonate stardust from the Murchison meteorite

*Kentaro Kudo[1]

1. TechnoPro, Inc. TechnoPro R&D Company

The formation of carbonates in meteorites is generally attributed to secondary aqueous alteration in “planetary environments” (such as Earth, Mars and asteroids), and carbonates are considered to be a good indicator of the past presence of liquid water. However, we report the first discovery of unique calcite grains embedded in the interior of a large calcium-aluminum-rich inclusion (CAI) from the Murchison CM2 carbonaceous chondrite. The individual calcite grains in the CAI are agglomerated submicron (<1 μm) crystals and coexist with high-temperature condensates such as spinel and diopside. The oxygen isotope ratios of the calcite grains have an extreme $^{17}O/^{16}O$ and $^{18}O/^{16}O$ anomaly and are clearly different from that of the secondary carbonates in the matrix. The calcite crystals have large negative anomalies with relatively heterogeneous oxygen isotope compositions ranging from −120 to +5‰ for $\delta^{17}O_{SMOW}$ and from −50 to +100‰ for $\delta^{18}O_{SMOW}$, which are extremely depleted in ^{17}O and enriched in ^{18}O relative to spinel and diopside (−45 to −40‰ for $\delta^{17}O_{SMOW}$ and −50 to −45‰ for $\delta^{18}O_{SMOW}$). Although the oxygen isotope compositions of the secondary carbonates are distributed along the TF line, those of the calcite grains in the CAI are heterogeneous and linearly distribute neither on the TF line nor near the TF line in the three oxygen isotope diagram. Therefore, our results suggest that the primitive carbonate grains may form in the proto-solar “nebular environment” without liquid water.

Keywords: Oxygen isotopes, Calcium-aluminium-rich inclusion, Molecular cloud, Proto-sun, Early solar nebula, Nano-SIMS

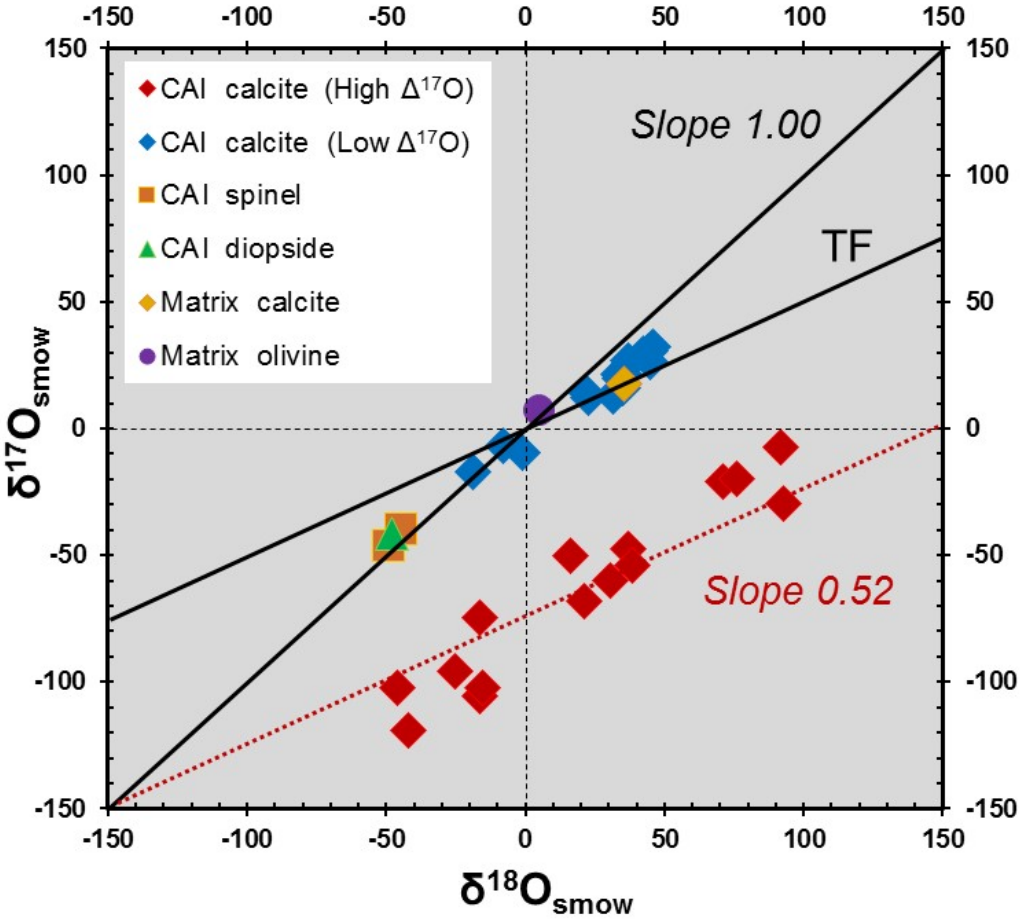

Variable shock deformation within the CV3 chondrites based on chondrule shapes determined by X-ray tomography and modes of chondrite components

*Ren Aoki[1], Timothy J. Fagan[1], Masayuki Uesugi[2], Akira Tsuchiyama[3]

1. Department of Resources and Emvironmental Engineering School of Creative Science and Engineering Waseda University, 2. Japan Synchrotron Radiation Research Institute, 3. Division of Earth and Planetary Sciences, Graduate School of Science, Kyoto University

Introduction: The high abundance of Fe,Ni-metal and high Fo-contents of olivine led to the recognition that the CV3 chondrites Efremovka, Leoville and Vigarano formed at relatively low oxygen fugacities as reduced CV3s (CV3red; [1,2]). In contrast, the CVs Allende and Axtell have little to no Fe,Ni-metal and are classified as an oxidized subgroup (CV3oxA). The CV3red subgroup is characterized by lower metamorphic grades and lower porosities than CV3oxA [3,4]. It has been proposed that the lower metamorphic grade of CV3red is due to an early impact event on the CV3 parent body that lowered porosities [5] and expelled ice [6]. In this study, we test the interpretation that the CV3red subgroup was preferentially deformed by shock by comparing (1) modes of chondrite components, (2) chondrule shapes and (3) clustering of chondrule orientations in a set of CV3red and CV3oxA chondrites.
Methods: We used elemental and BSE maps and photomicrograph mosaics of polished thin sections (pts) to determine modes of chondrite components (chondrules, CAIs, AOAs, matrix) in: one pts of Leoville; two pts of Efremovka; three pts of Vigarano; two pts of Allende and one pts of Axtell. We also determined 2-D shapes and orientations of chondrules in these pts.
Three-dimensional shapes and orientations of chondrules and chondrule-like objects were determined by X-ray computed tomography (CT) in small samples of Efremovka, Vigarano and Allende. X-ray CT data were collected using X-ray CT scanner at Kyoto University (ELESCAN, NX-NCP-C80-I; Nittetsu Elex Co.) [7]. The X-ray CT data consist of a series of 2-D images, in which pixel brightness correlates with linear attenuation coefficient (LAC) [7-8]. Elliptical shapes of low-LAC chondrules and chondrule-like objects were traced on a layer overlying each X-ray CT layer. The subsets of images of traced layers were processed using SLICE software [9] to investigate their shape using tri-axial ellipsoidal approximation and orientation of each axis of chondrules and chondrule-like objects in the samples.
Results: The ratios of matrix/inclusions ("inclusions" = chondrules + CAIs + AOAs) show a trend that correlates with the porosities of [4]. Matrix/inclusions ratios are near 0.3-0.4 for Efremovka and Leoville (porosities approx., 0.6-2%), 0.6-0.7 for Vigarano (porosity, 8%), and 0.9-1.0 for Allende (porosity, 22%). Our Axtell (porosity, 23% [4]) pts has matrix/inclusions ratio = 0.7, but a large CAI probably causes the ratio of the pts to be lower than that of Axtell as a whole. Ebel et al. [10] also found matrix/inclusions lower in Leoville and Vigarano than in Allende; however, their matrix/inclusions ratio for Allende (1.3) is higher than our results.
The 2-D pts data suggest and the 3-D X-ray CT data show that Allende chondrules tend to be spherical, and that the Efremovka and Vigarano chondrules tend to be oblate. Furthermore, the Efremovka and Vigarano chondrules have short axes with well-defined preferred orientations, consistent with flattening. The chondrite component modes, and chondrule shapes and orientations support the interpretation that the CV3red chondrites were affected by an early shock event that limited fluid-rock interaction during subsequent metamorphism [5,6]. Vigarano does not appear to be as strongly shocked as Efremovka and Leoville.
[1] McSween H.Y. (1977) GCA 41, 1777-1790. [2] Weisberg M.K. et al. (2006) *MESS 2*, Lauretta D.S. and McSween H.Y. (eds.) p. 19-52. [3] Bonal L. et al. (2006) GCA 70, 1849-1863. [4] Macke R.J. et al. (2011)

MaPS 46, 1842-1862. [5] Rubin A.E. (2012) GCA 90, 181-194. [6] MacPherson G.J. and Krot A.N. (2014) MaPS 49, 1250-1270. [7] Tsuchiyama A. et al. (2002) Geoch.J. 36, 369-390. [8] Uesugi M. et al. (2013) GCA 116, 17-32. [9] Nakano T. et al. (2006) Japan Synchrotron Radiation Research Institute. http://www-bl20.spring8.or.jp/slice/. [10] Ebel D.S. et al. (2016) GCA 172, 332-356.

Keywords: CV chondrites, shock deformation, X-ray tomography

Chondrule-cored aggregates (ChCAs): A new rock-type in CV chondrites with implications for timing of high-T crystallization events in the solar nebula

*Toshiki Yasuda[1], Timothy Fagan[1], Alexander N. Krot[2], Kazu Nagashima[2]

1. Waseda University, 2. University of Hawai'i

Introduction: Ca-Al-rich inclusions (CAIs) and amoeboid olivine aggregates (AOAs) formed by high-temperature reactions between gas and solids, and in some cases liquids, in a hot (ambient temperature > 1400K) region of the protoplanetary disk during initial stages of its evolution [1]. CAIs and AOAs in chondrites of petrologic types $\leq$3.0 tend to be ^{16}O-rich (Δ^{17}O -20‰). In contrast, chondrules formed at lower ambient temperatures (<900K) and tend to be ^{16}O-poor compared to CAIs (Δ^{17}O -10‰). Most chondrules appear to have postdated formation of CAIs and AOAs, though initial stages of chondrule formation might have overlapped with CAIs and AOAs [2,3]. Because of the later formation age of many chondrules, relict CAIs may be found included within chondrules [4], but chondrule fragments included in CAIs are very rare [5].

In this project, we describe minerals, textures and oxygen isotopes of three unusual objects from the CV3 chondrites Allende and Vigarano in which relict chondrule phenocrysts are partially enclosed by granular olivine texturally similar to AOAs. We refer to these objects as chondrule-cored aggregates (ChCAs). They are significant because their textures suggest the opposite of the conventionally accepted timing; namely, in ChCAs, an early stage of chondrule formation was apparently followed by a later stage of olivine condensation.

Methods: Two ChCAs (called NE-27 and SW-7) were identified in Allende, and one (NW-30) was found in Vigarano. Minerals and textures were characterized using petrographic microscopes, a scanning electron microscope (Hitachi S-3400N) and a JEOL JXA 8900 electron probe micro-analyzer (EPMA) at Waseda University. Oxygen isotopic compositions of olivine in the Allende ChCAs were collected using the Cameca ims-1280 SIMS at University of Hawai ‘i using conditions similar to those described in [6]. Typical uncertainty including internal and external errors is ~0.6‰ in both d^{17}O and d^{18}O.

Results: In Allende ChCA NE-27, a large (>200 μm across), low-Ca pyroxene ($En_{98}Wo_1$) similar to a chondrule phenocryst occurs in the core. The relict phenocryst is rimmed by granular olivine grains approximately < 20 μm across. The olivine grains are zoned with cores as Mg-rich as Fo_{95} and rims of approximately Fo_{60}. Olivines with compositions near Fo_{60} also occur in veins that cut across relict pyroxene. ChCA SW-7 has similar low-Ca pyroxene, granular olivine and vein olivine, but is composed of several nodules and has a more diffuse boundary with the Allende matrix. Vigarano ChCA NW-30 also has a core of low-Ca pyroxene. The granular olivine layer is not as complete as in the Allende ChCAs, but granular olivine does appear to replace low-Ca pyroxene near margins of ChCA NW-30.

SIMS oxygen isotope analyses of granular olivine from the Allende ChCAs fall near the Carbonaceous Chondrite Anhydrous Mineral and Primary Chondrule Mineral reference lines (see [7]) and form a spread of Δ^{17}O values from -8 to -3‰. All measurements are from MgO-rich cores and avoid FeO-rich olivine rims. The ^{16}O-poor isotopic composition indicates that the olivine rims of ChCAs did not form in a typical AOA-like setting. Regardless of O-isotopic setting, the ChCAs indicate (1) an early episode of chondrule formation, followed subsequently by (2) fragmentation or some process that released pyroxene phenocrysts from their host chondrules, (3) crystallization of granular olivine grains on the margins of relict phenocrysts, and (4) formation of Fe-rich olivine on rims of grains and in veins during metamorphism.

References: [1] Krot et al. (2009) GCA 73, 4963-4997. [2] Kita N.T. et al. (2005) in Krot et al. (eds) Chondrites and the Protoplanetary Disk, p. 558- 587. [3] Connelly et al. (2012) Science 338, 651-655. [4] Krot A.N. et al. (2007) MaPS 42, 1197-1219. [5] Itoh and Yurimoto. (2003) Nature 423, 728-731. [6] Nagashima K. et al. (2014) GCA 151, 49-67. [7] Ushikubo T. et al. (2012) GCA 90, 242-264.

Keywords: chondrules, solar nebula, oxygen isotopes

Development of Laser Post-Ionization SNMS for In-Situ U-Pb chronology

*Takahiro Matsuda[1], Yosuke Kawai[1], Kohei Miya[1], Jun Aoki[1], Toshinobu Hondo[1], Morio Ishihara[1], Michisato Toyoda[1], Ryosuke Nakamura[2], Kentaro Terada[1]

1. Graduate School of Science, Osaka University, 2. Office for University-Industry Collaboration, Osaka University

In space and planetary sciences, Secondary Ion Mass Spectrometer (SIMS) has been widely used for isotopic analyses at the micron scale. In the SIMS analysis, the surface of a sample is irradiated by a primary ion beam, and secondary ions of the sputtered materials are introduced into the mass spectrometer. However, the secondary ion yield of SIMS is very low (less than a few %). As a result, a large amount of material is wasted as neutral particles. In order to improve this disadvantage, we have been developing a Sputtered Neutral Mass Spectrometer (SNMS) with a femto-second laser.
The instrument consists of a focused ion beam system with a liquid metal gallium ion source (Ga-FIB) to attain an ultrahigh lateral resolution less than 1 μm. After a sputtering by Ga-FIB, the sputtered secondary particles are ionized by irradiating the femto-second laser. The post-ionized ions are introduced into the multi-turn ToF analyzer (MULTUM) which achieves ultrahigh mass resolving power of 20000. In addition, we introduced a new detection method, ion counting system, to improve the detection sensitivity. As a result of measurement of a standard sample in U-Pb chronology, 91500 zircon (concentration of uranium is about 100 ppm), the signal peaks of uranium and uranium oxides could be detected, so we have confirmed that the detection limit of the present system is 100 ppm.
In this study, we measured cyrtolite which contains a high concentration of uranium (2 wt.%) and 91500 zircon to confirm whether SNMS can be applied to in-situ U-Pb chronology. As a result of measuring two samples, uranium, uranium oxides and lead signal peaks were detected. In addition, signal peaks of interfering ions, for example, hafnium oxides and gallium clusters, were separated from the peaks of lead by increasing the number of cycles in MULTUM. After the measurement, the diameter of the sputtered area was about 1 μm. In this presentation, we will report the present performance of SNMS in in-situ U-Pb chronology.

Keywords: U-Pb chronology, SIMS, SNMS

Development of high precision Cr-Ti stable isotope measurements for extra-terrestrial materials.

*Yuki Hibiya[1], Tsuyoshi Iizuka[1], Katsuyuki Yamashita[2], Shigekazu Yoneda[3], Akane Yamakawa[4]

1. Graduate School of Science, The University of Tokyo, 2. Graduate School of Natural and Technology, Okayama University, 3. Department of Science and Engineering, National Museum of Nature and Science, 4. Center for Environmental Measurement and Analysis, National Institute for Environmental Studies

Introduction: Extra-terrestrial materials have highly variable $^{54}Cr/^{52}Cr$ and $^{50}Ti/^{47}Ti$ that do not follow mass-dependent fractionation. These variations are considered to reflect nucleosynthetic heterogeneities, possibly resulting from the incomplete and/or impermanent mixing of nuclides from different nucleosynthetic sources (e.g., 1-2). In recent years, these variations have become powerful tools for tracing astrophysical environments of early solar system (e.g., 3-4). They also provide important information about the genetic relationship between the planetary materials especially when the two isotope systems are combined (5). Here, we report the first sequential chemical separation procedure for high-precision Cr and Ti isotopic ratio measurements of extra-terrestrial rocks. We also measured Cr stable isotope compositions of the silicate samples processed through the new chemical separation scheme by thermal ionization mass spectrometry (TIMS).

Results & Discussion: Both Cr and Ti were successfully purified for standard rock samples basalt (JB-1b; 15-50 mg) and Juvinas (~20 mg) monomict non-cumulate eucrite using a new four-stage column chromatographic procedure. All the dissolved silicate samples were dried down, and re-dissolved in 2 mL of 6 M HCL for the first step of column chemistry. In the first step, Fe was separated from most elements including Cr and Ti using AG1-X8 anion exchange resin. The recovery rates in this step were 97-100% for Cr, ~100% for Ti, and 0% for Fe, respectively. In the second step, Ti-fraction was separated from Cr-fraction, and matrix elements like Ca were removed using AG50W-X8 cation exchange resin modifying the Ni separation procedure developed by (6). The recovery rates were 89-100% for Cr, 89-92% for Ti and 0% for Ca, respectively. In this step, Ti was about 43-66% left in the Cr-fraction, and Cr was about 1% left in the Ti-fraction. In the third step, Cr-fraction from the second step was further separated from Ti-fraction and purified for most matrix elements (V, Na, Mn, Mg, Na, Sr etc.) using AG50W-X8 cation exchange resin. The recovery rates in this step were 89-100% for Cr, 97% for Ti and 0% for most matrix elements. In this step, Ti and V were removed from the Cr-fraction, and about 1% of Cr and V left in the Ti-fraction. In the last step, Ti-fractions from the second step and the third step were combined, and the Ti-fraction was further purified for V and Cr. This chemical separation follows the procedure using TODGA resin described by (7). The recovery rates in this step were 97% for Ti, and 0% for Cr and V. These steps decrease the problematic isobaric interferences to be sufficiently low: $^{56}Fe/^{52}Cr$, $^{51}V/^{52}Cr$ and $^{49}Ti/^{52}Cr$ in Cr fraction were as low as 7.09×10^{-6}, 7.75×10^{-8} and 4.05×10^{-7}, respectively. The Cr stable isotope analyses yielded $\varepsilon^{54}Cr = 0.16 \pm 0.22$ (2SE) for JB-1b and $\varepsilon^{54}Cr = -0.48 \pm 0.25$ (2SE) for Juvinas. The reliability of the method was verified by the result that $\varepsilon^{54}Cr$ value for geostandard JB-1b is identical to that of Cr standard within the uncertainties. Furthermore, the $\varepsilon^{54}Cr$ value of Juvinas eucrite is identical within analytical uncertainty to the previous reported value ($\varepsilon^{54}Cr = -0.71 \pm 0.12$ (2SE); (8)). The sequential chemical separation scheme developed here allows us to extract Cr and Ti from basaltic samples with fewer steps than those in the previous study (e.g., 7,9) and with high recovery rates (>80% for all steps). We will apply the method to various extra-terrestrial materials for better understanding of the origin and evolution of the solar system.

References: (1) Trinquier et al. (2009), (2) Qin et al. (2011), (5) Warren, (2011), (6) Yamakawa et al. (2009), (7) Zhang et al. (2011), (8) Trinquier et al. (2007), (9) Schiller et al. (2014)

Keywords: Cr, Ti, nucleosynthetic anomaly, chemical separation, TIMS, eucrite

Development of integrated SR-CT method for the total analysis of meteorites

*Masayuki Uesugi[1], Akihisa Takeuchi[1], Kentaro Uesugi[1]

1. Japan synchrotron radiation research institute

Synchrotron radiation computed tomography (SR-CT) enables us to observe the internal structure of extraterrestrial materials with spatial resolution around 100nm three-dimensionally, without breaking them. In previous studies, however, we can not investigate the mineral phases and chemical composition of internal materials of the samples. In addition, considerable errors are occurred if we observed samples larger than the field of view of the CT instruments.

Recently, several methods of the combination of x-ray diffraction (XRD) and CT were developed in the material sciences of engineering fields [e.g. 1-2], and performed precise observation of polycrystalline metals or alloys. We can determine the mineral phases of the sample uniquely, orientation of the crystals inside them and analyze their chemical composition by linear attenuation coefficient [3].

In this paper, we report a new instrument for the total analysis of rocky material which includes XRD, SR-CT, and local tomography which images a region of interest of a sample by zooming up it. We also developed softwares for the integrated analysis of data obtained by the system. The software relates the images and data obtained by those different methods with simple operation. Using this system, we can search and investigate certain materials or minerals included in the sample, such as carbon phases. We also introduce future developments and application for analysis of materials obtained by future sample return missions.

References: [1] Toda et al., (2016) Acta Materialia 107 310-324. [2] West et al., (2009) Scripta Materialia 61 875–878. [3] Uesugi et al., (2013) Geochimica et Cosmochimica Acta 116, 17–32.

Keywords: synchrotron radiation tomography, XRD-CT, meteorite

3D-observation of matrix of MIL 090657 meteorite by absorption-phase tomography

*Sugimoto Miyama[1], Akira Tsuchiyama[1], Junya Matsuno[1], Akira Miyake[1], Tsukasa Nakano[2], Kentaro Uesugi[3], Akihisa Takeuchi[3], Aki Takigawa[1], Akiko Takayama[1], Keiko Nakamura-Messenger[4], Aaron S. Burton[4], Scott Messenger[4]

1. Division of Earth and Planetary Sciences, Graduate School of Science, Kyoto University, 2. AIST/GSJ, 3. JASRI/SPring-8, 4. NASA/JSC

MIL 090657 meteorite (CR2.7) is one of the least altered primitive carbonaceous chondrites [1]. This meteorite has amorphous silicates like GEMS (glass with embedded metal and sulfide), which are characteristically contained in cometary dust, in matrix [2,3] as with the Paris meteorite [4]. Three lithologies have been recognized; lithology-1 (L1) dominated by submicron anhydrous silicates, lithology-2 (L2) by GEMS-like amorphous silicates and lithology-3 (L3) by phyllosilicates [2]. Organic materials are abundant in L1 and L2 [2,3]. L1 and L2 were further divided into sub-lithology respectively based on their textures and compositions [5]. These studies were performed by 2D SEM and TEM observations of sample surfaces and thin sections that are unable to reveal what constitute each lithology and how these lithologies are distributed and related to each other. This information will provide important insights into alteration and aggregation processes on asteroids and in the early solar nebula.
In this study, MIL 090657 matrix was examined in 3D using two types of X-ray tomography; DET (dual-energy tomography) [6] and SIXM (scanning-imaging X-ray microscopy) [7]. Mineral phases can be discriminated based on absorption contrasts at two different X-ray energies in DET. In SIXM, materials composed of light elements such as water or organic materials can be identified based on phase and absorption contrasts. By combining these methods, we can discriminate not only organic materials from voids but also hydrous alteration products, such as hydrated silicates and carbonates, from anhydrous minerals [8].
In this study, we first observed cross sections of MIL 090657 matrix fragments (~100 mm) in detail using FE-SEM/EDS. Based on the results, three house-shaped samples (30~50 mm) were extracted from L1, L2 and their boundary (H1, H3 and H5, respectively) using FIB. 3D imaging of these samples were conducted at BL47XU of SPring-8, a synchrotron radiation facility, with ~30-40 nm/voxel and ~70-80 nm/voxel at 7keV and 8keV in DET and ~100 nm/voxel at 8keV in SIXM.
We found new lithologies that we named L4, L5 and L6 in H1 and H3 in addition to L1 and L2. L4. L5 and L6 are mainly composed of probably phyllosilicates with different Fe contents. Sulfide and framboidal magnetite were recognized in L4. L5 includes magnetite and carbonate and L6 includes anhydrous silicates having cracks inside. L1, L2, L4 and L5 are porous while few voids were observed in L6. L4 adjoins to L1 with boundary, which is not very distinct. L2, L5 and L6 adjoin to each other, and the boundaries of L6 with L2 and L5 are clear. In H5, coarse mineral grains (~5-10 mm) such as Fe-metal and enstatite are present in L1 and L2. L1-L2 boundary is not sharp in 3D.
In conclusion, we found a variety of lithologies by 3D observation for the first time, suggesting that the MIL 090657 meteorite experienced complex alteration and aggregation histories. As L2 is dominated by amorphous silicates, which are extremely susceptible to aqueous alteration, this is presumed to be the most primitive lithology. The contact between L2 and phyllosilicate-bearing lithologies (L5 and L6) with clear boundaries indicates that they were aggregated after aqueous alteration of L5 and L6. The indistinct boundary between L1 and L2 is suggesting that these two lithologies might originally be the same aggregate composed of amorphous silicates and coarse mineral grains. L1 might have experienced weak aqueous alteration followed by mild thermal alteration [2], while L2 did not undergo aqueous alteration.

[1] Davidson et al. 2015, 46th LPSC, 1603. [2] Cao et al. 2016, 47th LPSC, 2427. [3] Sugimoto et al. 2016, Goldschmidt Workshop on Experimental Cosmochemistry, 15. [4] Leroux et al. 2015, GCA, 170: 247-265. [5] Sugimoto et al. 2016, JAMS Ann. Congr. Abstr., 161. [6] Tsuchiyama et al. 2013, GCA, 116: 5-16. [7] Takeuchi et al. 2013, J. Synch. Rad., 20: 793-800. [8] Tsuchiyama et al. 2017, 48th LPSC, 2680.

Keywords: primitive carbonaceous chondrite, amorphous silicate, aqueous alteration

Reproduction of chondrules using ambient-controlled levitation system

*Yusuke Seto[1], Kouta Suzuki[1], Naoki Shoda[1]

1. Graduate School of Science, Kobe University

Chondrules are round (or irregular) shaped particles with sizes ranging of 0.1 −10 mm. They are mainly composed of silicates, iron metals and iron sulfides, and thought to be formed by the rapid cooling of fully or partially molten droplets before they accreted. They show unique and diverse internal micro-textures (e.g., porphyritic olivine, barred olivine, radial pyroxene, etc.) which reflect not only a composition of the stating material, but also nebular conditions, such as gas species and their partial pressures, heating and cooling rate. The conditions of chondrule formation, however, remain poorly constrained. This is mainly because the reproduction of the chondrule formation processes in a laboratory is experimentally difficult, especially in terms of a container-less arrangement and a reducing (low-fO2) ambient. In the present study, we developed gas-levitation system embedded in ambient-controlled tube furnace in order to reproduce micro-textures of chondrules, and to constrain their formation conditions.
A summary of the newly developed equipment is as follows. A vertical tube furnace with a silicon carbide heater (double coiled spiral type) and an alumina core tube (OD 50mm, ID 42 mm, referred to as “outer-tube” hereafter) was used as a heating device. An alumina inner core tube (OD 32mm, ID 26 mm, referred to as “inner-tube” hereafter) was inserted into the outer tube, and an amorphous-carbon gas-nozzle (blowout hole diameter of 1 mm) was set on at the top of the inner-tube. H_2+CO_2+Ar mixed gas were separately introduced into the both inner and outer core tubes from a gas port at the bottom of the tubes, and gas flow rates were controlled by digital mass flow controllers. The inner tube with the gas-nozzle can move up and down by a motor-controlled pantograph, and thereby the seamless switching from a sample exchange positon to maximum temperature position is possible. Levitated samples were observed by a long focal CCD camera thorough mirrors and infrared filters. To avoid lowering of the image contrast due to incandescence above 1500 K, area around the sample were irradiated by a system of high-power LED (20W) and large-aperture lens.
Using the above system, we demonstrated the containerless cooling experiments for molten silicate droplets. As stating materials, (i) natural peridotite (analogue to a Fe-poor chondrule) and (ii) oxide mixture corresponding to a type IIA (F-rich) chondrule were used. They were melted at (i) 1773 K and (ii) 1673 K for durations of ~5 min and cooled with a rate of 10^4 K/hr under a reducing condition (log fO2 = IW-1) in the above system. Surfaces and internal textures of the recovered samples were analyzed using SEM-EDX. In the recovered samples of (i), residues of original olivine (Fa~10) were surrounded by overgrown Fe-poor olivine (Fa6) with zigzag surfaces. In the molten area, both platy (10 μm thickness) and porphyritic (3-20 μm) olivines were observed. Both of them showed distinct chemical zoning and are embedded in Al_2O_3-SiO_2-rich glass. The samples of (ii) were thought to be experienced by fully molten states. They shows also both platy (100 μm thickness) and porphyritic (10-30 μm) olivine embedded in an Al_2O_3-SiO_2-rich glass. Although previous studies suggest that porphyritic chondrules were formed from partially molten states while nonporphyritic chondrules from fully molten states, the present results indicates that porphyritic texture is still possible to be formed from fully molten states. The demonstrations of the present study show that reducing-gas levitation experiments is a powerful technique to simulate the molten-quenched texture of early solar materials.

Keywords: chondrule, gas levitation , quench texture

Occurrence of Fe in sulfides, silicates and metals in enstatite and ordinary chondrites: Wide ranges in oxidation-reduction due to variations in H_2O gas?

*Yuki Tanimura[1], Timothy Fagan[1]

1. Department of Earth Sciences, School of Education, Waseda University

Introduction: Iron is one of the most abundant elements in solid materials of the solar system, and occurs in chondrites in 3 main mineral groups: silicates, metals, and sulfides [1]. Speciation of Fe between these mineral groups is an indicator of the conditions where chondrites formed in the solar nebula.
Fe-speciation of chondrites between silicates and metal indicates wide variations in oxidation state [1]. Were there similar variations in the extent of sulfidation? In this project, we use Fe speciation among silicates, metal, and sulfides in enstatite, ordinary and Rumuruti-like chondrites to address variations in oxidation, reduction and sulfidation in the part of the solar nebula where these chondrite groups formed.
Methods: We used elemental and BSE maps of polished thin sections (pts) to determine modes of minerals (enstatite, olivine, Fe,Ni-metal, troilite,…) in: Bensour (LL6), Mt. Tazerzait (L5), Tamdakht (H5), LEW 88180 (EH5), NWA 974 (E6), NWA 953 (R3). Elemental maps were collected using a JEOL JXA-8900 electron probe micro-analyzer (EPMA) at Waseda University (WU). Modes were determined manually using grids overlain on the pts maps in a graphics program. The compositions of major minerals were analyzed using the WU EPMA. We calculated moles of Fe in each mineral using the mineral compositions, published molar volumes and the modes.
We also used wet chemical analyses of chondrite whole rocks from two data sets: one collected and compiled by the Smithsonian Museum, US [2], and the other by the National Institute of Polar Research (NIPR), Japan [3]. In these analyses, FeO, Fe-metal and FeS were determined directly.
A reaction space approach [4,5] was used to identify the main reactions possible between minerals and O- and S-rich gas in E, O and R chondrites. The reacting system consists of the following phases and solid solution vectors: $NaAlSi_3O_8$, $CaMgSi_2O_6$, $MgSiO_3$, $AlAlMg_{-1}Si_{-1}$, SiO_2, O-rich gas, S-rich gas, $FeMg_{-1}$, Fe-metal, FeS, $CaAlNa_{-1}Si_{-1}$ and Mg_2SiO_4. These phases can be described by the components: Na, Ca, Mg, Al, Si, O_2, S_2 and Fe. In this system, all transfers of mass between the silicate, sulfide and metal subsystems can be described as progress along two reactions: (R_m) $Mg_2SiO_4 + 2\ FeMg_{-1} = 2\ Fe + SiO_2 + O_2$; and ($R_s$) $Mg_2SiO_4 + 2\ FeMg_{-1} + S_2 = 2\ FeS + SiO_2 + O_2$. Increasing reduction is indicated by progress on R_m, increasing sulfidation by progress on R_s, and oxidizing conditions are indicated by minor progress on both reactions. Progress on R_m is designated by X_m and ranges from 0 to 1; likewise, X_s shows progress on R_s.
Results: Fe-speciation determined from all three data sets indicate wide variations in FeO/Fe-metal (X_m from 0 to 1) and limited variations in FeO/FeS (X_s mostly from 0.1 to 0.3). The results from most oxidized to most reduced are: R-, LL-, L-, H-, E-chondrites, in agreement with [1].
Considering a model for flow of ice and other materials in the solar nebula [6], the extent of oxidation was high at an evaporation front. In this model, evaporation of H_2O-ice caused the local gas to become enriched in H_2O, increasing the oxygen fugacity of the gas. With more oxygen present in the gas, R_m could proceed to the left, transferring Fe from metal to silicates. The R chondrites could have formed just inside of the evaporation front, where the gas was enriched in H_2O-vapor. Ordinary and enstatite chondrites might have formed farther inward from the evaporation front.
References: [1] McSween H.Y. and Huss G.R. (2010) *Cosmochemistry,* Cambridge, 217-218. [2] Jarosewich E. (2006) MaPS 41:1381-1382. [3] Yanai K. and Kojima H. (1995) *Catalog of the Antarctic Meteorites*, NIPR, 230 p. [4] Thompson J.B. et al (1982) JPetrol vol. 23: 1-27. [5] Fagan T.J. and Day H.W.

(1997) Geology 25: 395-398. [6] Cuzzi J.N. and Zahnle K.J. (2004) AstrophysicalJ vol. 614: 490-496.

Keywords: chondrites, solar nebula, oxidation-reduction

Shock pressure estimation by high-pressure polymorphs and cathodoluminescence spectra of maskelynite in Yamato-790729 L6 chondrite and their significance for collisional condition

Yukako Kato[1], Toshimori Sekine[1,2], *Masahiro KAYAMA[1,3,4], Masaaki Miyahara[1,3], Akira Yamaguchi[5,6]

1. Department of Earth and Planetary Systems Science, Graduate School of Science, Hiroshima University, 2. Center for High Pressure Science and Technology Advanced Research, 3. Department of Earth and Planetary Material Sciences, Faculty of Science, Tohoku University, 4. Creative Interdisciplinary Research Division, Frontier Research Institute for Interdisciplinary Sciences, Tohoku University, 5. National Institute of Polar Research, 6. Department of Polar Science, School of Multidisciplinary Science, SOKENDAI

Most asteroidal meteorites have experienced impact events that occurred on their parent-bodies because shock-induced features (e.g., melting textures, high-pressure polymorphs and vitrification) provide clear evidences for impact events. L6 type ordinary chondrite frequently has a vein-like shock-induced melting texture (a shock-melt vein or shock vein). Furthermore, they may contain high-pressure polymorphs and shock-induced glasses (e.g., maskelynite) that were transformed from the constituent minerals (e.g., olivine, pyroxene and plagioclase) due to high-pressure and –temperature conditions induced by impact events. Such high-pressure polymorphs and shock-induced glasses provide constraints on the asteroidal impact history. In this study, Yamato (Y)-790729, which is classified as heavily shocked L6 type ordinary chondrites, was investigated to estimate the shock-pressure, temperature and size of the parent body, based on high-pressure polymorph assemblage and cathodoluminescence (CL) spectroscopy of maskelynite. The shock pressure conditions estimated by these two methods were also compared each other to evaluate the validity of the methods.

Y-790729 is a typical L6 ordinary chondrite with remnants of chondritic textures, and has a shock-melt vein. The host-rock of Y-790729 consists mainly of olivine, low-Ca pyroxene, feldspar, metallic Fe-Ni, and iron-sulfide with minor phosphate and chromite. Undulatory extinction was recognized in some plagioclase and pyroxene grains under the optical microscope. A scanning electron microscope (SEM) , laser micro-Raman spectroscopy and transmission electron microscope (TEM) equipped with an X-ray energy dispersive spectrometer (EDS) were carried out for this meteorite to determine the chemical composition, observe the petrological features and identify the high-pressure phases. Another SEM with a CL spectrometer was also conducted to characterize the shock metamorphic effects of the feldspar and maskelynite.

A shock-melt vein with a width of < ~620 μm exists in Y-790729. TEM observations and micro-Raman spectroscopy of this meteorites demonstrated that ringwoodite, majorite, akimotoite, lingunite, tuite, and xieite occurred in and around the shock-melt vein. The ringwoodite is polycrystalline assemblages under the TEM observations, where the individual grain reaches from ~0.1 to ~1.3 μm across. According to the phase equilibrium diagrams of these high-pressure polymorphs, the shock pressure in the shock-melt vein is about 14-23 GPa.

Part of plagioclase grains in the host-rock occurred as maskelynite under the optical microscope and Raman spectroscopy. Sixteen different CL spectra from maskelynite portions of Y-790729 showed characteristic emission bands at ~330 and 380 nm. The obtained CL spectral data of maskelynite portions were deconvoluted into three emission components at 2.95, 3.26, and 3.88 eV. The intensity of emission component at 2.95 eV was selected as a calibrated barometer to estimate shock pressure, and the results indicate shock pressures of about 11-19 GPa. The difference in pressure between the shock-melt vein and host-rock might suggest heterogeneous shock conditions.

Assuming an average shock pressure of 18 GPa, the impact velocity of parent-body of Y-790729 is calculated to be ~1.90 km/s. The melting temperature of the shock vein could be about 2173 K at 18 GPa, according to previous data obtained from the KLB-1 peridotite and Allende meteorite. It is likely that the duration of high-pressure and -temperature conditions recorded in the shock-melt veins of Y-790729 is several seconds, implying that the parent-body size is ~ 10 km in diameter at least, based on the incoherent formation mechanism of ringwoodite in Y-790729.

Keywords: L6 type ordinary chondrite, Yamato-790729, high-pressure polymorphs, cathodoluminescence

Discovery of heavily shocked type 3 ordinary chondrites

*Masaaki Miyahara[1], Akira Yamaguchi[2], Eiji Ohtani[3]

1. Department of Earth and Planetary Systems Science, Graduate School of Science, Hiroshima University, 2. NIPR, 3. Department of Earth Sciences, Graduate School of Science, Tohoku University

Based on the onion cell model, a parent-body of an ordinary chondrite consists of petrographic type 6, 5, 4 and 3 from inward to outward. A high-pressure polymorph occurring in a shocked ordinary chondrite gives shock pressure, temperature, impact velocity and impactor size, which become clues for understanding a destruction process of an ordinary chondrite parent-body. We have to clarify the inventories of a high-pressure polymorph included in all petrologic types to elucidate the destruction process of an ordinary chondrite parent-body. Accordingly, we will describe the petrologic and mineralogical features of the shock-induced textures and high-pressure polymorphs therein in heavily shocked type 3 ordinary chondrites.

We observed about three hundreds Antarctica type 3 ordinary chondrite (H-, L- and LL-type) petrographic thin sections stored in the NIPR under an optical microscope. We found eight type 3 ordinary chondrites with a distinct melting texture; Y-981139 (H3), A-87170 (L3), A-87220 (L3), Y-000886 (L3), Y-86706 (L3), Y-981327 (L3) A-881199 (LL3.4) and A-881981 (LL3). We also selected thirty three type 3 ordinary chondrite petrographic thin sections without a melting texture as a reference. All these samples were scanned with a field-emission scanning electron microscope (FE-SEM) to observe the fine-textures of melt-pockets and the morphologies of chondrules. Mineralogy was determined by a laser micro-Raman spectroscopy.

FE-SEM observations revealed that the melting textures (melt-pocket) in type 3 always occur around a boundary between a chondrule and matrix. Fine-grained quench silicate crystals and the spherules of metallic iron-nickel + iron sulfide with a eutectic texture filled the melt-pockets. Several interstitial glass fragments were entrained in the melt-pockets of A-881199 (LL3). Their bulk-chemical compositions are similar to that of plagioclase. Based on a Raman spectroscopy analysis, most of them are amorphous. On the other hand, back-scattered electron (BSE) image depicted that one of the interstitial glasses had a granular texture. A strong Raman shifts appeared at 372, 693 and 1032 cm-1 from the interstitial glass with a granular texture, which appear to be those of jadeite (Considering its chemical composition, probably, jadeite-diopside solid-solution) or tissintite. This is a first discovery of a high-pressure polymorph from type 3 ordinary chondrite. The ellipticity of chondrules (1 −(short axis/long axis)) in type 3 chondrites with and without a melting texture was measured. The ellipticity of chondrules in chondrites with a melting texture is ˜0.31, which appears to be a bit bigger than those of chondrules in chondrites without a melting texture. The orientation of the long axis of chondrules was also measured. The long axis of chondrules in chondrites with a melting texture appears to be oriented along a specific orientation. The ellipticity and orientation degree of chondrules besides a high-pressure polymorph would be available for estimating shock pressure condition recorded in an ordinary chondrite.

Keywords: ordinary chondrite, shock, high-pressure polymorph

Formation process of Fe-FeS globules in melt veins in shocked ordinary chondrites

*Riho Tani[1], Naotaka Tomioka[2], Kaushik Das[1]

1. Hiroshima University Department of Earth and Planetary Systems Science, 2. Kochi Institute for Core Sample Research, Japan Agency for Marine-Earth Science and Technology

Heavily shocked stony meteorites contain optically black veins called shock veins. The veins consist of micron to submicron-scale grains of silicates, oxides, Fe-Ni metals and Fe-sulfide. During shock vein formation, metal-sulfide melt is not chemically mixed with silicate melt due to their mutual immiscibility. As a result, the metal-sulfide is crystallized as tiny globules in the silicate/oxide matrix in shock veins. Such globules are an unequivocal evidence for extensive melting of silicate materials. Previously, mineralogical studies of shock vein have been mainly focused on silicate and oxide minerals, since these minerals often occur as high-pressure phases. Pressure-temperature histories in shocked chondrites have been deduced from high-pressure mineral assemblages based on experimentally determined phase equilibria [1]. However, metals and sulfides in shock veins have not been well investigated. In the present study, we have examined the Fe-FeS globules in shock veins in two ordinary chondrites (NWA4719 and Tenham), which are considered to have experienced different shock pressures, [2–3] to obtain further information of the formation process of shock veins.

The trend of the globule size in the shock vein shows that it becomes larger from the vein wall to the center (up to 25 μm) due to the difference of cooling rate and local fluid dynamics. Following the previous study [4], cooling rates of shock veins were estimated from spacing of Fe-metal dendrites in the globules by a cooling-rate meter established for Fe-dendrites in alloys [5]. The widths of Fe-dendrites in NWA4719 and Tenham are in the range of ~300–600 nm, and estimated cooling rates of the shock veins in are extremely high (10^6 deg C/sec).

To evaluate such a seemingly unrealistically high cooling rate, we examined mineral phases of the globules in Tenham by TEM/STEM. Fe-FeS globules are surrounded by high pressure silicate minerals including aluminous majorite crystallized from chondritic melt at pressures above 14 GPa. Meanwhile, X-ray elemental mapping clarified that the globules consist of grains of kamacite, taenite and troilite (<2 μm in size). But, high-pressure phases of Fe-sulfide such as Fe_3S_2 and Fe_3S, which are stable above ~14 and ~21 GPa [6,7] respectively, were not found. The results suggest that shock pressure in Tenham was significantly dropped from >14 GPa when temperature of the shock vein was in between the liquidus temperature of silicate (~2000 deg C) and eutectic temperature of Fe-FeS (~1000 deg C). Therefore, only silicate minerals could have been crystallized as high pressure phases. The absence of high-pressure phases of Fe-sulfide is rather consistent with much slower cooling rate than that estimated by Fe-dendrite spacing. The cooling-rate meter established in metallurgical studies provides overestimated values for shock veins formed in a dynamic high-pressure process.

References: [1] e.g. Agee et al. (1995) J. Geophys. Res. 100, 17725–17740. [2] Kimura et al. (2007) Meteorit. Planet. Sci. 42, 5139.pdf. [3] e.g. Tomioka and Fujino (1999) Am. Mineral. 84, 267–271. [4] Scott (1982) Geochim. Cosmochim. Acta 46, 813–823. [5] Flemings et al. (1970) J. Iron Steel Inst. 208, 371-381. [6] Fei et al. (1997) Science 275, 1621–1623 [7] Fei et al. (2000) Am. Mineral. 85, 1830–1833.

Keywords: metal-sulfide globule, shock vein, ordinary chondrite, TEM

Petrologic evidence for early impact events inferred from differentiated achondrites

*Akira Yamaguchi[1], Naoki Shirai[2]

1. National Institute of Polar Research, 2. Tokyo Metropolitan University

Eucrites, grouped in the HED meteorites are the largest group of differentiated achondrites. There are several achondrites petrologically similar to eucrites but were derived from distinct sources. Detailed petrologic and geochemical studies of such asteroidal achondrites provide better understanding of early igneous, thermal and impact histories of differentiated planetesimals. We report petrology and geochemistry of achondrites, EET 92023 and Dho 007. Oxygen isotopic compositions of these meteorites are significantly shifted away from the eucrite fractionation line. EET 92023 is an unbrecciated achondrite whereas Dho 007 is a polymict breccia mainly composed of medium to coarse-grained granular clasts. These achondrites are mainly composed of low-Ca pyroxene and plagioclase, petrologically similar to normal cumulate eucrites. However, these rocks contain significant amounts of kamacite and taenite not common in unbrecciated, crystalline eucrites. EET 92023 and Dho 007 contain significant amounts of platinum group elements (PGEs) (~10% of CI), several orders of magnitude higher than those of monomict eucrites. We suggest that the metallic phases carrying PGEs were incorporated by projectiles during or before igneous crystallization and thermal metamorphism. The projectiles were likely to be iron meteorites rather than chondritic materials, as indicated by the lack of olivine and the presence of free silica. Therefore, the oxygen isotopic signatures are indigenous, rather than due to contamination of the projectile materials with different oxygen isotopic compositions. A significant thermal event involving metamorphism after the impact event indicates that EET 92023 and Dho 007 record early impact events which took place shortly after the crust formation on a differentiated protoplanet when the crust was still hot.

Keywords: meteorites, achondrites

A petrographic study of the NWA 2924 mesosiderite

*naoji sugiura[1], makoto kimura[2], tomoko arai[1], takafumi matsui[1]

1. Chiba Institute of Technology, 2. ibaraki University

Recent chronological studies [1,2] revealed that reheating of mesosiderites occurred significantly later (~30 Ma) than the solidification of the magma ocean (~4563 Ma) on the parent body. At this age, 26-Al cannot be a significant heat source. Also, metal cannot be the heat source because even if it was derived from a core, its composition should have been fractionated by this time. (Mesosiderite metal is not fractionated in siderophile elements.) Therefore, an alternative heat source has to be looked for. Here we report petrography of a mesosiderite which was largely molten by the reheating event, based on which we discuss the heating process.

NWA 2924 has not been studied in detail. But it is noteworthy that it suffered only minor shock effects (Meteoritical Bulletin). Two polished sections (one metal nodule and one matrix) were observed with a SEM and the mineral compositions were analyzed with an EDS. The areal silicate fractions are plagioclase=0.380, pyroxene=0.534 and silica=0.086. This corresponds to the type A mesosiderite. Sub-classification of mesosiderites by degrees of reheating is rather confusing [3]. In our opinion, melt-rock mesosiderites should be classified as type 3. (Type 4 is eliminated.) They can be easily distinguished from type 2 by the absence of olivine coronas and by the presence of silica/plagioclase needles that penetrate into metal. By this definition, NWA 2924 is a type 3A mesosiderite.

Chromite in NWA 2924 shows three types of petrographic features. (1) Some chromites contain ubiquitous spherical silicate inclusions. (2) Some chromites contain similar spherical silicate inclusions which are restricted to the outer part of the chromite grains. (3) Clusters of smaller chromite grains which do not include much silicate inclusions are present. Such clusters are often observed in silicate inclusions inside metal nodules. The spherical silicate inclusions are considered to be produced as follows. Chromite and surrounding silicates were heated to above the solidus temperatures of silicates, and chromite was dissolved into the silicate melt. Shortly afterwards, it cooled rapidly and silicate melt was trapped in the growing chromite. In case (1), the heating was just enough for complete melting of chromite. In case (2), only the outer part of chromite was dissolved. In case (3), chromite was completely dissolved and the dissolved chromite component diffused away considerably, so that new chromite grains formed upon individual nucleation sites (that are located nearby), resulting in a cluster of small chromites. Such chromite features are different from those in shock-heated chondrites [4]. In shocked chondrites, chromite appears as fine (micron size) granular fragments because it is brittle.

This petrographic observation is important in 3 ways. First, it suggests that the heating was very brief. Second, it seems that chromite in metal nodules was molten more extensively, suggesting different environment such as higher temperatures and/or different melt compositions and volumes than the matrix. Third, shock heating is an unlikely mechanism for reheating mesosiderites, although it may be preferred solely based on the briefness of the heating.

Since radiogenic heat, accreting hot metal and shock heating are all ruled out as a heat source for mesosiderite reheating, we suggest that induction heating due to changing solar-wind magnetic field (joule heating by eddy current) is a plausible mechanism for mesosiderite reheating. We certainly need more observations of chromite in melt-rock mesosiderites and other shocked meteorites.

[1] M.Koike et al., G.R.L. 2017, in press. [2] M.K. Haba et al., 79th Metsoc, 2016, #6139. [3] R.Hewins, J.G.R.1984, 89, C289-C297. [4] X.Xie et al., Eur. J. Mineral. 2001, 13, 1177 - 1190.

Keywords: mesosiderite, reheating, induction

The consideration regarding formation environment of the nakhlite meteorites inferred from deformation microstructures

*Amiko Takano[1], Ikuo Katayama[1], Tomohiro Usui[2], Motoo Ito[3], Katsuyoshi Michibayashi[4]

1. Hiroshima University, 2. Earth-Life Science Institute, Tokyo Institute of Technology, 3. Kochi Institute for Core Sample Research JAMSTEC, 4. Institute of Geosciences, Shizuoka University

The nakhlite is classified as one of the Martian meteorites, and are interpreted to have originated from the Tharsis region (Treiman et al., 1987). In contrast to the Earth’ s rock, the nakhlite meteorites crystallized in thick lava flows (>125m) or in shallow intrusion (probably less than a kilometer depth), however, the details of the formation environment is still unknown (Treiman et al., 1987). Therefore, it is important to investigate the formation process and environment of the nakhlite based on comprehensive observations of crystallographic orientations in constituting minerals.
In this study, we examined a polished thin section of the Yamato 000593 nakhlite (Y000593) by mineralogical, textural and crystallographic observations using an optical microscope and electron probe micro analyzer (EPMA) at Hiroshima University and scanning microscope combined electron backscatter diffraction (SEM-EBSD) at Shizuoka University.
The Y000593 mainly composed of augite, olivine and mesostasis that is consistent with previous reports for nakhlites (e.g., Mikouchi et al., 2003). The lattice-preferred orientations for minerals in whole rock of the meteorite were determined from EBSD patterns for understanding of deformation under metamorphic conditions. We found that Y000593 has crystal preferred orientation patterns in clinopyroxenes. It is suggested that the shear stress had acted on to augites when they crystallized. Thus, we inferred the nakhlites deposited in some kind of flows such as a stream of lava that flows out of a volcano.
On the other hand, we considered the impact effect when Y000593 was ejected from Mars. In general, pyroxenes are good indicator of shock deformation, which induces mechanical twins as one of the examples of crystal defects (e.g., Mori and Takeda 1983). To estimate the effect of impact process, we measured the mechanical twin planes, which were observed in many augites in Y000593. Consequently, most of augites with mechanical twin have been formed on (100) planes. This mechanical twin is known to induce deformation in clinopyroxenes at high strain rates and moderate temperatures (Leroux et al., 2004). In comparison with the microstructural observations in experimentally shocked clinopyroxene to the results of Y000593, it is suggested that the Y000593 pyroxenes are not strongly shocked and affected by impact event. This result is consistent with a previous study that has demonstrated impact effect using degree of extinction in olivine and pyroxene in Martian meteorites (Fritz et al., 2005).

Keywords: nakhlite, crystal preferred orientation, formation environment, impact effect

Hydrogen Reservoirs in Mars as Revealed by SNC Meteorites

*Tomohiro Usui[1]

1. Earth-Life Science Institute, Tokyo Institute of Technology

The isotopic signatures of three hydrogen reservoirs are now identified based on analyses of Martian meteorites, telescopic observations, and Curiosity measurements: primordial water, surface water, and subsurface water (Usui, in press). The primordial water is retained in the mantle and has a D/H ratio similar to those seen in Martian building blocks (Usui et al. 2012). The surface water has been isotopically exchanged with the atmospheric water of which D/H ratio has increased through the planet's history to reach the present-day mean value of ~5,000‰ (Kurokawa et al. 2014). The subsurface water reservoir has intermediate δD values (~1,000-2,000‰), which are distinct from the low-δD primordial and the high-δD surface water reservoirs. We proposed that the intermediate-δD reservoir represents either hydrated crust and/or ground ice interbedded within sediments (Usui et al. 2015). The hydrated crustal materials and/or ground ice could have acquired its intermediate-δD composition from the ancient surface water reservoir (Usui et al. 2017).

References:

Kurokawa, H. et al. (2014). Evolution of water reservoirs on Mars: Constraints from hydrogen isotopes in martian meteorites. *Earth Planet. Sci. Lett.* **394**, 179-185.

Usui et al. (2012) Origin of water and mantle-crust interactions on Mars inferred from hydrogen isotopes and volatile element abundances of olivine-hosted melt inclusions of primitive shergottites. *Earth Planet. Sci. Lett.* **357-358**, 119-129.

Usui et al. (2015) Meteoritic evidence for a previously unrecognized hydrogen reservoir on Mars. *Earth Planet. Sci. Lett.* **410**, 140-151.

Usui et al. (2017) Hydrogen isotopic constraints on the evolution of surface and subsurface water on Mars. The *48th Lunar Planetary Science Conference*, Abstract #1278.

Usui et al. (in press) Hydrogen reservoirs in Mars as revealed by SNC meteorites. *Volatiles In The Martian Crust* (eds. Filiberoto J. and Schwenzer S. P.), Elsevier B.V.

Keywords: hydrogen isotope, Martian meteorites

Variations in Shock Deformation of Feldspars in Three Achondrites: NWA 2727 Lunar breccia, NWA 856 Shergottite and NWA 3117 Howardite.

*Jaeyong Lee[1], Timothy Fagan [2]

1. Department of Environmental Studies, Graduate School of Frontier Sciences, The University of Tokyo, 2. Department of Earth Sciences, School of Education, Waseda University

In this study, I investigated shock history and geochemistry of three achondrite meteorites: NWA 3117, a howardite breccia from asteroid 4 Vesta; NWA 2727, a breccia from the Moon; and NWA 856, a shergottite from Mars. Shock histories of the three meteorites were evaluated from deformation of plagioclase feldspars. Geochemical study focused on electron microprobe (EPMA) analyses of pyroxene grains and use of Mn/Fe ratios to verify classification of these samples. Feldspar grains were classified based on observations in cross-polarized light as undulatory, mosaic, mosaic-recrystallized or maskelynite. This sequence represents increasing deformation of original feldspar crystals. Undulatory crystals have wavy extinction, mosaic crystals have patchy extinction, and mosaic-recrystallized grains appear as if they were originally coarse-grained and have recrystallized to mosaics of small equant crystals. Maskelynite grains are isotropic, indicating transformation to glass. Based on feldspar deformation, the degrees of impact processing are NWA 856 > NWA 3117 > NWA 2727. All of the feldspar observed in NWA 856 is maskelynite; mosaic and mosaic-recrystallized feldspars are common in NWA 3117; and the feldspar in NWA 2727 tends to have undulatory extinction.
The high deformation of NWA 856 is expected because this sample is from Mars, which is a large parent body and requires a powerful impact to accelerate a rock to escape velocity. In contrast, the parent body of NWA 3117 (Vesta) is smaller than that of NWA 2727 (the Moon), yet NWA 3117 appears more highly deformed than NWA 2727. One possible explanation is that NWA 2727 is from a relatively young part of the Moon, which has not been exposed to impacts as long as the surface of Vesta. My EPMA analyses of pyroxenes show that Mn/Fe ratios are highest in NWA 3117, lower in NWA 856, and lowest in NWA 2727, and are consistent with classification of these meteorites as a howardite (parent body Vesta), shergottite (Mars), and lunar meteorite (Moon), respectively. The higher volatility of Mn vs. Fe suggests that the observed variations in Mn/Fe could result from parent body formation at temperatures that were highest for the Moon, lower for Mars, and lowest for Vesta. However, variations in oxygen fugacity and other parameters may also have affected Mn/Fe.

Keywords: Howardite, Shergottite, Lunar breccia, Shock deformation, Feldspar, EPMA Analysis

Validation on the scenario of the formation of asteroid belt by deuterium fusion explosion of Jupiter-like planet

*Shinji Karasawa[1]

1. Miyagi National College of Tecnology Professor emeritus

A celestial body more than 1.3% of the mass of the Sun can begin temporary fusion of deuterium [1]. Gravitational potential energy of the center of this celestial body calculated under the constant density corresponds to the temperature on deuterium is about one million degrees (10^6K). The celestial body will blast when the amount of substances emitted from the celestial body by deuterium fusion is larger than the gas being sucked by gravity.
The planet for the validation is 13 times mass of Jupiter. Orbit of the model is the same with Ceres (the center of asteroid belt:4.14x10^8 km). Distances between planets and the Sun are as follows. Neptune:45.04, Uranus:28.75, Saturn:14.29, Jupiter:7.78, planet (X):4.14, Mars:2.27, and Earth:1.50. [in 10^8 km unit]. Gravitational field of each planet was calculated at the point of the same gravity with the Sun. Values are Neptune: 0.32, Uranus: 0.19, Saturn: 0.24, Jupiter: 0.24, planet (X): 0.81, Mars: 0.013, and Earth: 0.026 [in 10^8 km unit]. Planet (X) is located at a little outside of the snow line (4.04x10^8 km [2]). Gravitational collapse is progressed in a short time due to existence of hydrogen gas about 100 times mass of dust. So, planet (X) became very large.
About 4.6 billion years ago, the Sun began the nuclear fusion. At that time, substances of solid core of the Sun were ejected into universe. Those had accelerated the growth of the planet (X). After that, the planet (X) began deuterium fusion. But, it was ended in an only blast. Most of fragments of planet (X) were emitted in the universe. Although debris that keeps the same orbital speed remains in the asteroid belt, the movement of gravitational center does not change due to elastic collision. Heavy bombardment of meteorites at 3.8 billion years before can be explained by deuterium fusion explosions of planet (X).
Further descriptions are presented at website: “https://youtu.be/QY8C7XK6k7I”, “https://youtu.be/fiMgXpUz2GQ”.

[References]

[1] Chabrier, G., Baraffe, I., Low-mass stars and substellar objects, Ann. Rev. Astron. Astrophys. 38 (2000) 337-377.
[2] Hayashi, C., Prog. Theor. Phys. Suppt., Vol. 70, pp. 35-53.

Keywords: asteroid belt, meteorite, deuterium fusion, brown dwarf, Jupiter, Ceres

Effects of protoplanetary multiplicity and migration on late-stage accretion of solids onto gas giants

*Sho Shibata[1], Masahiro Ikoma[1], Yuhiko Aoyama[1]

1. Graduate School of Science, The University of Tokyo

In recent years, many extrasolar gas giants have been discovered, and detailed observation reveals common characteristics of those gas giants. Their envelopes are thought to have come from protoplanetary disks, whose composition must be almost the same as that of central stars, namely, composed mainly of hydrogen and helium. Several studies of the bulk composition of gas giants, however, indicate that the envelopes of many gas giants, including Jupiter and Saturn, are much richer in heavy elements than the central stars. To explain the origin of the heavy elements, previous studies performed N-body simulations of planetesimals around growing gas giants and estimated the amount of heavy elements captured by gas giants. The estimated total masses are about a few Earth masses, which are too small to explain the observation. In this study, for the effects that enhance solid accretion, we take the multiplicity and migration of protoplanets into account. We demonstrate that the existence of another protoplanet can help supplying planetesimals to the protoplanet by scattering and also protoplanetary migration enhances the capture of planetesimals by sweeping. As a result, since planetesimals in broader area are captured by the planet, the envelopes end up being richer in heavy elements than previously thought.

Keywords: Heavy Elements, Planet Formation, Extrasolar Planet

Mystery of Planetary Integration Mechanism, and Origin of Moon,Asteroid Belt,Core Rich Mercury, Mystery and all Origins were unified proved by Application of Abduction at One-case Evolution with “Multi-Impact Hypothesis” to Past.

*Akira Taneko[1]

1. SEED SCIENCE Lab.

Titius Bode's law is an unenviable heuristic.However, this law has suggested the requirements of the collision coalescence of the planet each other.
When the particles of the circular orbital and the elliptical orbit are tangential collision with almost no speed difference at the far point position, they coalesce and speed decreases by thermal energy.
According to Titius Bode's law the orbital radius is expressed as Rn = Re ×(o.a + 0.4 ×2 $^{(n-1)}$). However, Re ≈149 597 870.700 km: one astronomical unit n=1 Mercury, n =2 Venus, n =3 Earth. n =4 Mars, n =5 Ceres, n =6 Jupiter, n =7 Saturn, n =8 Uranus⋯.It comes to doubt in this neighborhood
In the simulation of the giant impact hypothesis, the moon formation of only the mantle component was calculated, but the moon's orbital energy was only 1/20 of the actual one. In Abduction 's way of thinking you can explain the current situation, reliability will increase, but if you cannot explain it will increase suspicion.
In the multi impact hypothesis, since we were able to explain all of the origins of plate tectonics, the deep sea floor and the Pacific arc islands origin and the eccentricity of the Van Allen belt and the new driving force of plate tectonics in a unified way, It can be said that it could be verified by evolution and history.
In addition, ***the multi impact hypothesis*** can also explain the origins of the asteroid zone, the origin of the differentiated meteorites, the origin of Jupiter's great red spots and Pluto, the inclination of Neptune's axis, and the large origin of Mercury's core-mantle ratio. In addition to explaining the origin and evolution of the solar system in a unified way. Elucidation of the origins in the solar system physics is impossible to reproduce and it is difficult to elucidate by induction or deduction.However, if we use a physically meaningful hypothesis, the origin of the solar system also matched the initial conditions It can be said that it is closer to the truth because it can be verified by using abductions completely systematically with multiple current situations using one-time evolution.

In the simulation of hypothesis relying on no basis, there are few results and many contradictions are obtained.
In particular, in **the giant impact hypothesis**, we cannot explain the difference in density between the front and back of the moon and the origin of the meteorite heavy bombing period.
All origins can be elucidated by abduction, other proofs are difficult.
In the multi impact hypothesis, furthermore, the origin of the asteroid belt and the planetary blank of the Sera position, the core / mantle ratio of Mercury is twice that of other earth type planets, the origin of Jupiter 's large red spot, the origin of Pluto, the origin of diamond The origins of the kimber light pipe, the mysteries of the differentiated earth meteorite, the mystery of the plate movement direction sudden change, etc. can all be explained unifiedly

Keywords: Planetary accumulation mechanism, Origin of the asteroid belt, Origin of the Moon, Origin of Large Red Spot, Differentiated asteroids, core rich Mercury

チチウス･ﾎﾞｰﾃﾞの法則を再検討 (2)

8.チチウス･ボーデの法則の問題点, 8-1.本仮説での証明方法

種子彰 2016

◆水星 n＝-∞この理由が説明できない. ⇒ 禁制帯とマルチインパクト仮説.

◆小惑星帯 n＝3の欠番理由が説明できない. ⇒ CERRAの潮汐関断裂.

◆海王星 n＝7での不一致と, 冥王星の一致の理由が説明できない. ⇒CERRA断裂片のフライバイと海王星衝突

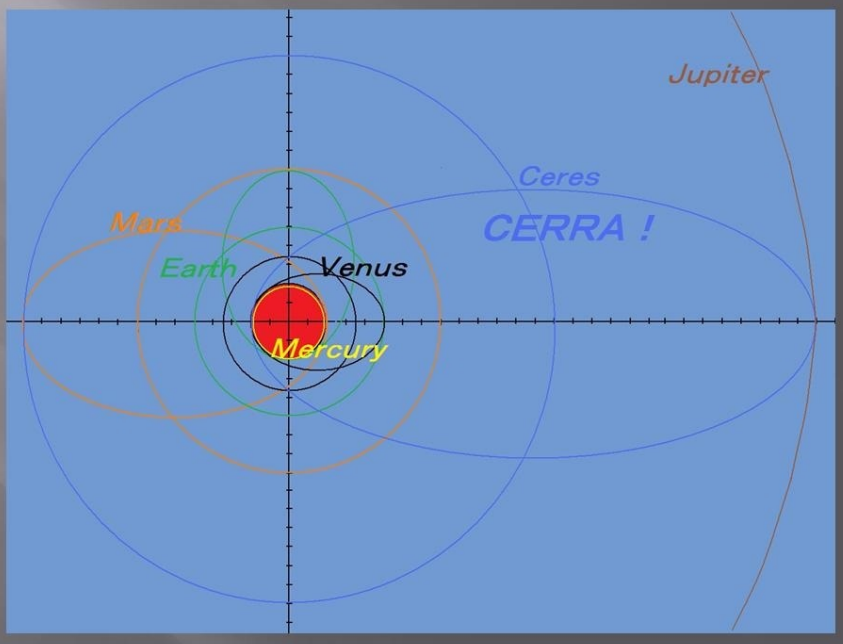

8-1.＜証明＞

●禁制帯,フィーデングゾーンでの合体

●微惑星楕円軌道道近点での衝突合体による軌道縮退

●CERRAの潮汐断裂片⇒水星に.

●断裂片木星スイングバイ⇒冥王星